

γ -ray emission associated with cluster-scale AGN outbursts

J. A. Hinton,^{1*} W. Domainko² and E. C. D. Pope¹

¹*School of Physics and Astronomy, University of Leeds, Leeds LS2 9JT*

²*Max-Planck-Institut für Kernphysik, Heidelberg D 69029, Germany*

Accepted 2007 August 29. Received 2007 June 12; in original form 2006 November 6

ABSTRACT

Recent observations have revealed the existence of enormously energetic $\sim 10^{61}$ erg active galactic nuclei outbursts in three relatively distant galaxy clusters. These outbursts have produced bubbles in the intracluster medium, apparently supported by pressure from relativistic particles and/or magnetic fields. Here, we argue that if \geq GeV particles are responsible then these particles are very likely protons and nuclei, rather than electrons, and that the γ -ray emission from these objects, arising from the interactions of these hadrons in the intracluster medium, may be marginally detectable with instruments such as the Gamma-ray Large Area Space Telescope (GLAST) and the High Energy Stereoscopic System (HESS).

Key words: galaxies: active – galaxies: clusters: general – gamma-rays: theory.

1 INTRODUCTION

Galaxy clusters are the largest gravitationally bound systems in the Universe. In addition, radio (Giovannini & Feretti 2000; Feretti et al. 2004) and hard X-ray (Rephaeli & Gruber 2002; Fusco-Femiano et al. 2004) observations have revealed that a significant component of non-thermal particles can be found in such systems. The remaining tracer of non-thermal particles is high-energy (HE) γ -ray emission, but no such signal has been firmly detected from galaxy clusters so far (Reimer et al. 2003).

Despite this non-detection, a number of arguments suggest that galaxy clusters are potentially powerful emitters of HE radiation. Völk, Aharonian & Breitschwerdt (1996) and Berezhinsky, Blasi & Ptuskin (1997) recognized that hadronic cosmic rays (CRs) with energies of less than 10^{15} eV accumulate within the cluster volume for the entire Hubble time. This CR component, together with the presence of target material in the form of the hot intracluster medium (ICM), will lead to very high energy (VHE) γ -ray production via inelastic proton–proton collisions and subsequent π^0 decay (Dennison 1980; Völk et al. 1996). Furthermore, leptonic CRs are also capable of generating HE electromagnetic radiation: TeV electrons may upscatter cosmic microwave background (CMB) photons to γ -ray energies in the inverse Compton processes (Atayan & Völk 2000; Gabici & Blasi 2003, 2004). The lifetime of VHE electrons, however, is limited by intracluster (IC) and synchrotron losses to $\sim 10^6$ yr (for typical cluster magnetic field strengths). Therefore, only recently injected electrons will contribute to the production of VHE γ -rays. Finally, if populations of ultra HE ($> 10^{18}$ eV) CR protons exist in galaxy clusters, they will interact with CMB photons and produce electron–positron pairs which will in turn radiate TeV

photons (with a characteristically hard energy spectrum) via the IC mechanism (Inoue, Aharonian & Sugiyama 2005).

Several sources of CRs are plausible in galaxy clusters. Large-scale shock waves caused by hierarchical structure formation may accelerate particles to sufficiently HEs (Colafrancesco & Blasi 1998; Loeb & Waxman 2000; Ryu et al. 2003). Additionally, supernovae and galactic winds from cluster galaxies can populate galaxy clusters with non-thermal particles (Völk et al. 1996). Furthermore, powerful active galactic nuclei (AGN) are believed to be prominent injectors of CRs into the ICM (Enßlin et al. 1997; Aharonian 2002; Pfrommer & Enßlin 2004).

In this paper, we focus on the scenario where a powerful AGN injects HE particles into a galaxy cluster. Prominent AGN are often found in galaxy clusters with short-central cooling times of the thermal ICM (for a review of these so-called *cooling flow clusters* see Fabian 1994) and their effect on the ICM can be seen in several systems (see Birzan et al. 2004, for a sample of such galaxy clusters). High-resolution X-ray observations have revealed bubbles, cavities and weak shocks in the ICM driven by activity of the central galaxy in several systems (e.g. Böhringer et al. 1993; Blanton et al. 2001; McNamara et al. 2001; Schindler et al. 2001; Fabian et al. 2003; Choi et al. 2004). Bubbles in the X-ray gas are often associated with radio lobes, indicating the presence of relativistic electrons (Owen, Eilek & Kassim 2000; Fabian et al. 2002; Gitti et al. 2006). Very recently, so-called *cluster-scale* AGN outbursts have been found in three clusters, all with estimated mechanical energy of at least 10^{61} erg. These systems are: MS 0735.6+7421 (McNamara et al. 2005), Hercules A (Nulsen et al. 2005a) and Hydra A (Nulsen et al. 2005b; Wise et al. 2007). Large-scale radio emission was found in Hydra A with deep very large array observations (Lane et al. 2004). Due to the large amount of energy input into these systems by the central AGN, plausibly in the form of relativistic particles, these systems may be promising targets for high- (and very high) energy γ -ray observations.

*E-mail: j.a.hinton@leeds.ac.uk

Table 1. Characteristics of powerful AGN outbursts. The flux F'_ν is calculated under the assumption of *Scenario A* (discussed later).

Object	z	$P_{\text{ext}}V$ (10^{61} erg)	Age (10^8 yr)	Mean density n_e (10^{-3} cm $^{-3}$)	Bubble diameter (kpc arcsec $^{-1}$)	$\nu F'_\nu$ (100 GeV) (10^{-13} erg cm $^{-2}$ s $^{-1}$)
MS 0735.6+7421	0.22	6	1.0	3	240/70	0.7
Hercules A	0.154	3	0.6	5	160/55	1.2
Hydra A	0.0538	0.9/0.41	1.4	5	210/200	3.0

Experimentally, γ -ray astronomy is in a phase of rapid development. Several Imaging Atmospheric Cherenkov Telescopes (IACTs) have recently been completed: HESS (Hinton 2004), Major Atmospheric Gamma-ray Imaging Cherenkov (Telescope) (Lorenz 2004) and the Very Energetic Radiation Imaging Telescope Array System (Krennrich et al. 2004). The combination of these VHE instruments with the HE detector GLAST (Thompson 2004), due for launch early next year, will provide sensitive coverage of the 100 MeV to 10 TeV energy regime for the first time. Here, we will argue that these instruments may be close to the sensitivity threshold required to detect the HE electromagnetic signatures of large-scale AGN outbursts in galaxy clusters.

In this paper, we investigate the HE luminosity of the three known galaxy clusters which host cluster-scale AGN outbursts. The relevant properties of these systems are given in Table 1.

2 COSMIC RAYS IN CLUSTER-SCALE OUTBURSTS

The existence of radio synchrotron emission in coincidence with X-ray cavities seen in AGN outbursts indicates the existence of relativistic electrons within the bubbles and leads naturally to the suggestion that relativistic particles may support these cavities. This hypothesis must be confronted with three key issues: (i) can relativistic particles be confined for the required time-scales?; (ii) are the energy loss time-scales of these particles sufficiently long? and (iii) is there observational evidence for other contributions to the bubble pressure?

For cluster-scale outbursts the time-scales involved have been estimated at $\sim 10^8$ yr, considerably longer than for previously identified systems (Birzan et al. 2004). Fig. 1 shows the relevant energy loss time-scales for ultrarelativistic electrons in the central cluster environment. We find that for the typical B -fields of a few μG found in the central regions of clusters, TeV electrons lose their energy on time-scales of 10^6 yr via inverse Compton and synchrotron cooling (see Fig. 1). Only $< \text{GeV}$ electrons can exist at the outer edge of a bubble of age $\sim 10^8$ yr. The observed radio synchrotron emission should therefore provide evidence for spectral cooling away from the central AGN. In the case of Hydra A, this spectral steepening is clearly seen (Lane et al. 2004). The measurements are broadly consistent with the injection of a power law of electrons ($dN/dE \propto E^{-\alpha}$) with $\alpha \sim 2$ which is subsequently cooled above a critical energy $E_{\text{crit}} \sim 100$ MeV to $\alpha \sim 3$ (resulting in radio synchrotron spectral index of ~ 1). By considering continuous injection and synchrotron cooling of the electrons over the lifetime of the outburst, we estimate that the currently radio emitting electrons represent roughly one-third of the total energy injected in electrons over this period. To estimate the energy carried by these electrons, an estimate of the magnetic field strength inside the bubbles is required. Rotation measure estimates of the magnetic field *outside* the radio lobes of Hydra A suggest $B \sim 30 \mu\text{G}$ (Taylor & Perley 1993). If the B -field within the lobes is similar then the total energy in electrons, and in the magnetic field itself, are both close to 10^{59} erg. As the

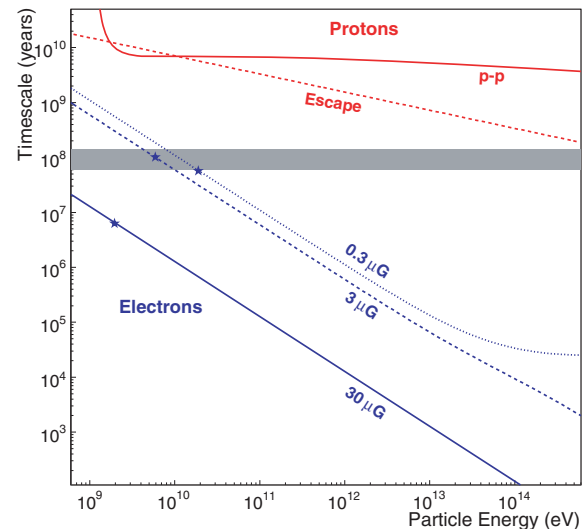


Figure 1. Time-scales of relevance to AGN outbursts. For protons, the mean time between inelastic collisions (solid line) and the escape time from the system (dashed line, assuming diffusion as given by equation (9) of Völk et al. (1996) with $B = 3 \mu\text{G}$), are shown. Note that this is the escape time from a 100 kpc radius bubble, the time required to escape the cluster (under the same assumptions) is $\sim 10^{10}$ yr for a 10^{15} eV proton. For electrons, the energy loss time-scale ($E/(dE/dt)$) due to synchrotron and inverse Compton radiation is shown for three different magnetic field strengths. The stars show the mean electron energy contributing to 1 GHz synchrotron emission for the three different field strengths. An ambient density of 5×10^{-3} protons cm^{-3} is assumed. The target photon field for inverse Compton scattering is taken solely as the CMB. This is then an upper limit on the cooling time-scale, since infrared photons from the central galaxy may also act as targets for the inverse Compton process. The shaded band indicates the apparent ages of the outbursts considered here.

total energy associated with the Hydra-A outburst is $\sim 10^{61}$ erg it seems that at least in this system there is missing pressure within the bubbles unless the magnetic field strength there is $\gg 30 \mu\text{G}$. To support the Hydra-A bubbles solely with magnetic pressure requires $B \sim 300 \mu\text{G}$. Such high fields seem unlikely due to the observation of smooth features in the 1.4 GHz emission on ~ 100 kpc scales. The synchrotron cooling time of the 1.4 GHz emitting (500 MeV) electrons in a $300 \mu\text{G}$ field is such that rectilinear propagation at speeds very close to c would be required to reach the edge of these features. The missing pressure may be ascribed to thermal gas (Gitti et al. 2007) or hadronic CRs (Dunn & Fabian 2004). We note that in the past proton dominated jets have been suggested (Celotti & Fabian 1993; Sikora & Madejski 2000) injecting hadronic CRs into the ICM during AGN outbursts. CR protons and nuclei have much less severe energy losses than electrons. For a proton to electron ratio of only 1/30, these particles could provide the energy required to support the bubbles. Furthermore, the escape time of $< 10^{15}$ eV protons from the central 200 kpc of these clusters is likely to be longer than the lifetime of the bubbles (Völk et al. 1996). A large

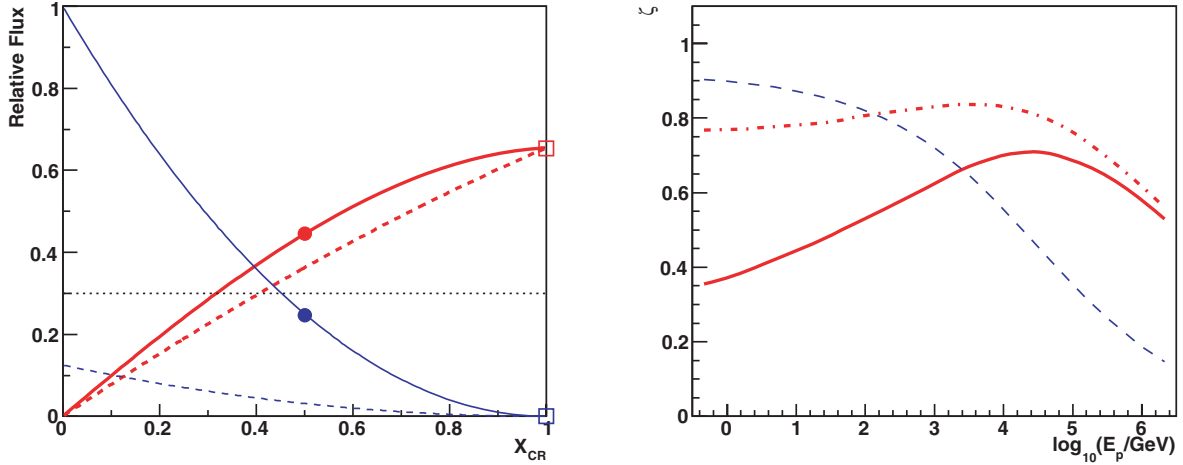


Figure 2. Left-hand panel: relative flux of X-rays and γ -rays as a function of the relative CR pressure X_{CR} . The X-ray flux from inside the bubbles (thin falling lines) is expressed relative to that of an equal volume of gas at the temperature and the pressure of the external medium. The γ -ray flux from the system is shown relative to that expected for a density contrast $\eta = 1$. Two cases are shown: $T_{\text{int}} = T_{\text{ext}}$ (solid line) and $T_{\text{int}} = 4T_{\text{ext}}$ (dashed line). The dotted horizontal line indicates the approximate range of X-ray contrast excluded by observations. Right-hand side: the energy dependence of CR confinement within the bubbles (dashed line) and the mixing parameter ζ for two assumptions for X_{CR} and T_{int} , $X_{\text{CR}} = 0.5$, $T_{\text{int}} = T_{\text{ext}}$ (dash-dotted curve, indicated by solid circles in the left-hand panel) and $X_{\text{CR}} = 1.0$ (solid curve, indicated by open squares in the left-hand panel). In both panels, the system geometry, external density profile and diffusion coefficient are specific to the Hydra-A system. Low-energy particles do not penetrate far into the external medium, and hence encounter mostly low-density gas inside the bubble. At the highest energies, CRs begin to escape from the high-density parts of the cluster into the more tenuous ICM. Note that the CRs with $\log_{10}(E/\text{GeV}) = 4$ are those primarily responsible for the 1 TeV γ -ray emission.

fraction of the injected CRs may therefore be confined within the observed bubbles for the required 10^8 yr (see Fig. 1) but the particles with the highest energies are likely able to penetrate the thermal gas which surrounds the bubbles (see Fig. 2). We further note that in cluster-scale AGN outbursts, the central black hole must accrete a significant fraction of its own mass in a single activity period and convert it very efficiently into mechanical power (McNamara et al. 2005; Nulsen et al. 2005a,b). Therefore, there is not much room for additional radiative energy losses of the relativistic particles driving the observed shock fronts.

For Hydra A it therefore seems likely that thermal gas or hadronic CRs dominate the bubble pressure.¹ For the other objects considered here such detailed radio observations do not exist. In general, magnetic fields and/or low-energy electrons can be considered viable alternatives as the dominant energy content of AGN jets (see e.g. De Young 2006; Dunn, Fabian & Celotti 2006).

Assuming that hadronic CRs are primarily responsible for the bubble expansion, two additional inputs are needed to calculate the γ -ray flux from these objects. First, an estimate of the internal energy in CRs at the present day and secondly, an estimate of the target density in and around the bubbles. Both these numbers require consideration of the hydrodynamics of the outbursts, which are discussed in the next section.

3 BUBBLE PROPERTIES

From the X-ray data, we can determine, or constrain, many properties of the AGN-inflated bubbles. Observations of the

¹ We note that this conclusion rests on the extrapolation of the observed radio spectrum in Hydra A down to <400 MeV electron energies (i.e. radio frequencies below 74 MHz). Electrons of a few hundred MeV have long enough lifetimes to support the bubbles, and could have sufficient energy if there is a second spectral component at these energies.

X-ray surface brightness profile yield the pressure of the gas outside the bubble, the bubble volume and limits to the emissivity of the material inside the bubble. This evidence indicates that the density of bubble material is low compared to its surroundings.

It is probably reasonable to assume an approximate pressure balance between the material inside the bubble and the ambient gas. Therefore, the external pressure is balanced by the total pressure exerted by the sum of the partial pressures of each component in the bubble: thermal pressure (P_{th}), CR pressure (P_{CR}), magnetic pressure (P_{mag}) and the relativistic electron pressure (P_{elec}). However, the radio data indicate that, in the case of Hydra A, the magnetic and the electron partial pressures are likely less significant than the thermal and CR components. Henceforth, we will consider the bubble to be a mixture of only thermal material and CRs and define $X_{\text{CR}} = P_{\text{CR}}/P_{\text{ext}}$, where P_{ext} is the external pressure on the bubble. In this case, the total internal energy content within the bubble volume V is

$$E_{\text{int}} = V \left(\frac{P_{\text{th}}}{\gamma_{\text{th}} - 1} + \frac{P_{\text{CR}}}{\gamma_{\text{CR}} - 1} \right), \quad (1)$$

where $\gamma_{\text{th}} = 5/3$ is the adiabatic index of the thermal material and $\gamma_{\text{CR}} = 4/3$ is the adiabatic index of the relativistic CRs. In this description, the density inside the bubble is governed by P_{CR} and the temperature of the material. We note that the case of overpressurized bubbles $X_{\text{CR}} > 1$ may be greater than 1.

Another useful parameter, when discussing the properties of bubbles, is the density contrast (η) between the material within the bubble ρ_{bub} and the ambient material ρ_{ext} , $\eta = \rho_{\text{ext}}/\rho_{\text{bub}}$. It should be noted that the CRs make a negligible contribution to ρ_{bub} . If we consider a jet that injects CRs and hot gas at a constant rate, then if this inflates a bubble, the average density within the bubble is

$$\rho_{\text{bub}} = \frac{\dot{m}t}{V(t)}, \quad (2)$$

where \dot{m} is the mass injection rate of the jet and $V(t)$ is the time-dependent volume of the cavity. The enthalpy of a slowly inflated

bubble is

$$E = L_{\text{jet}} t = \frac{\gamma}{\gamma - 1} P_{\text{ext}} V(t), \quad (3)$$

where L_{jet} is the constant jet power and γ is the effective adiabatic index, such that

$$\frac{\gamma}{\gamma - 1} = \frac{\gamma_{\text{th}}}{\gamma_{\text{th}} - 1} (1 - X_{\text{CR}}) + \frac{\gamma_{\text{CR}}}{\gamma_{\text{CR}} - 1} X_{\text{CR}}. \quad (4)$$

Therefore, we see that the volume of the bubble is proportional to the duration of the AGN outburst. Consequently, since the mass injection rate is also constant, so must be ρ_{bub} . Combining equations (2) and (3), and substituting $P_{\text{ext}} = k_{\text{b}} T_{\text{ext}} \rho_{\text{ext}} / \mu$, gives the density contrast,

$$\eta = \frac{\gamma - 1}{\gamma} \frac{\mu L_{\text{jet}}}{\dot{m} k_{\text{b}} T_{\text{ext}}} \quad (5)$$

which depends on the jet parameters and the temperature of the ambient gas. Assuming a constant mass injection rate, η increases for greater jet power because the density of material within the bubble is lower. η is roughly constant (and $\gg 1$) whilst the jet is active. After the jet switches off and the bubble rises buoyantly, it will expand to maintain pressure equilibrium with its surroundings, and the density contrast will fall. We can obtain a simple description of this by assuming that the bubble behaves adiabatically. Under adiabatic conditions, the specific entropy of the bubble will remain constant, thus,

$$\frac{P_{\text{bub}}}{\rho_{\text{bub}}^\gamma} = \text{constant}. \quad (6)$$

Since the temperature of the ICM is roughly constant with radius, $P_{\text{ext}} \propto \rho_{\text{ext}}$, and the bubble is in pressure equilibrium with its surroundings, we have: $\rho_{\text{bub}} \propto \rho_{\text{ext}}^{1/\gamma}$ and $\eta \propto \rho_{\text{ext}}^{1-1/\gamma}$. Thus, the density of the bubble falls less steeply than that of the ICM.

The argument above describes the slowest possible rate at which η can approach unity. In practise, bubbles probably behave far from adiabatically. Analysis of recent hydrodynamic simulations using the FLASH code suggests that the Kutta–Zhukovsky force plays an important part in mixing the bubble with the ICM and dissipating the bubble enthalpy over a relatively short time-scale (Pavlovski et al. 2007).² These simulations show that η approaches a value of 1, from an initial value of 1000, after rising only a few bubble radii. The observed X-ray contrast of the bubbles can be used to place limits on the density inside the bubbles for a given temperature. The X-ray contrast is approximately $(n_{\text{int}}/n_{\text{ext}})^2 (T_{\text{int}}/T_{\text{ext}})^{1/2}$. The uncertainties on the X-ray measurements and the geometry of the bubbles are such that this quantity must be less than about approximately one-third for the Hydra-A system (Wise et al. 2007). Fig. 2 shows this X-ray contrast as a function of the relative CR pressure X_{CR} for two different assumed temperatures T_{int} .

In the context of this work, it is also important to know the density of material in the bubble rim. In the early stages, the bubble inflation is likely to be highly supersonic, meaning that the density of the rim material should be roughly four times denser than the ambient material. Since the emissivity is proportional to the square of the gas density, this will lead to the appearance of bright rims surrounding bubbles. However, because the cooling time of these

rims is short compared to that of the surrounding gas, the rims are expected (and observed, see Blanton 2004; Gitti et al. 2007) to be cold ($kT \ll 1$ keV). Using the cooling function given by Sutherland & Dopita (1993), we find that the time taken to cool from 4 keV (the approximate temperature of the gas 100 kpc from Hydra A) to $\ll 1$ keV is: $t_{\text{cool}} \approx 1.4 \times 10^8 (n_0/10^{-2} \text{ cm}^{-3})^{-1} (kT_0/4 \text{ keV})^{1.5}$ yr. Assuming a compression ratio of four, the rims in these systems would have a density $2 \times 10^{-2} \text{ cm}^{-3}$, and hence cool in about half the age of the observed bubbles.

4 MODEL

As discussed in the previous sections, we assume here that hadronic CRs are responsible for expanding the observed bubbles. To calculate the rate of proton–proton interactions and the secondary particle production in these interactions, we apply the parametrizations derived by Kelner et al. (2006) based on the SIBYLL hadronic interaction model (Fletcher et al. 1994). Adapting Kelner et al. (2006) equation (69), the flux of γ -rays from proton–proton (and nucleus–nucleus) interactions can be expressed as:

$$\frac{dN_\gamma}{dE_\gamma} = \kappa n_e c V \epsilon(E_\gamma) \times \int_{E_\gamma}^{\infty} \zeta(E_p) \sigma_{\text{pp}}(E_p) \frac{dn_p}{dE_p} f_\gamma(E_\gamma/E_p, E_p) \frac{dE_p}{E_p} \quad (7)$$

κn_e is the effective cross-section weighted number density of target (thermal) protons and nuclei (a thin target approximation is appropriate as $t_{\text{pp}} \gg t_{\text{bubble}}$). Assuming a primordial abundance of both CRs and target nuclei, we find $\kappa = 1.15$. c is the speed of light, V is the bubble volume, $\epsilon(E_\gamma)$ represents the γ - γ absorption on the (infrared) extragalactic background light (EBL). We note that following recent constraints from the HESS (Aharonian et al. 2006) and *Spitzer* Dole et al. (2006) instruments, uncertainties on the EBL in the relevant wavelength range are now greatly reduced. Here, we calculated EBL absorption $\epsilon(E_\gamma)$ using the wavelength-dependant ($z = 0$) EBL density given in fig. 13 of Dole et al. (2006), ignoring evolutionary effects. The function $\zeta(E_p)$ reflects the degree of mixing between the target nuclei and the CRs. $\zeta = 1$ corresponds to the case of CRs confined in a uniform medium with electron density n_e . $f_\gamma(E_\gamma/E_p, E_p)$ is the energy distribution function for γ -rays produced in an average interaction of a proton of energy E_p (see equation 56 of Kelner et al. 2006). The spectral energy density of protons is assumed to be of the form:

$$\frac{dn_p}{dE_p} = k E_p^{-\alpha} \exp\left(\frac{-E_p}{E_{\text{max}}}\right). \quad (8)$$

With k chosen such that $V \int_{1 \text{ GeV}}^{\infty} dn_p/dE_p = E_{\text{CR}} = 3 P_{\text{ext}} V X_{\text{CR}}$. Diffusive shock acceleration, either relativistic (see e.g. Kirk et al. 2000) or non-relativistic, predicts a spectral index of injected particles close to two. We therefore set $\alpha = 2$ for the purpose of our calculations. The predicted peak flux (in the GeV range) varies only weakly with the assumed energy range. In contrast, the predicted TeV emission depends strongly on the maximum energy of the injected particles. The value of at least $E_{\text{max}} = 10^{14}$ eV (as assumed here) is required to produce up to 10 TeV γ -rays. Higher values, common to many predictions of hadron acceleration in AGN jets (see e.g. Biermann & Strittmatter 1987), do not significantly increase the > 10 TeV emission due to the absorption of higher energy photons on the EBL.

The spectrum of the injected secondary electrons is calculated in a similar way to that of γ -rays. The time evolution

² This force acts to expand the bubble radially, but perpendicularly to the direction of ascent. As the bubble expands an additional component of the Kutta–Zhukovsky force pushes the bubble down, reducing its ascent velocity (Landau & Lifschitz 1995).

of the secondary electron spectrum is followed in small time-steps accounting for synchrotron losses and injection via p–p interactions.

The estimation of the quantity $\zeta(E_p)$ introduced above is key to evaluating the fluxes from these objects. $\zeta(E_p)$ depends on the energy-dependent transport of CRs and on the density profile of the bubbles. An estimation of the density profile in turn requires an estimation of the fraction of the bubble pressure provided by CRs (X_{CR}), and hence the remaining pressure provided by hot gas. The left-hand panel of Fig. 2 shows the relative expected X-ray flux (from inside the bubbles) and the total γ -ray flux (from inside and outside the bubbles) as a function of X_{CR} , for two different assumed internal temperatures. X-ray fluxes above the dashed horizontal line are effectively excluded by the observed X-ray contrast of the bubbles. The CR spatial distribution is derived by a numerical transport simulation of energy-dependent diffusion assuming the value suggested by Völk et al. (1996) equation (9), combined with advection. Note that for the purpose of the diffusion calculation, a magnetic field inside and outside the bubbles was assumed to be the same. In general, the diffusion inside the bubbles is much more uncertain and could have a significant effect on the observed γ -ray flux. The right-hand panel of Fig. 2 shows (dashed line) the fraction of CRs confined within the bubble under these assumptions. Integrating over this curve, the total CR energy inside the bubbles is 74 per cent. The remaining curves on Fig. 2 (right-hand panel) show $\zeta(E_p)$ calculated numerically for the two cases marked on Fig. 2 (left-hand panel): $X_{\text{CR}} = 0.5$, $T_{\text{int}} = T_{\text{ext}}$ (dash-dotted curve, solid circles in the left-hand panel of Fig. 2) and $X_{\text{CR}} = 1.0$ (solid curve, indicated by open squares in the left-hand panel Fig. 2). For these calculations, we assume external density profile based on X-ray measurements (see fig. 4 of Nulsen et al. 2005b) and bubble rims with a compression ratio of 4. It can be seen that at HEs ($> \text{TeV}$), the results are rather insensitive to the internal density of

the bubbles, as most emission arises from the regions just outside the bubbles.

5 RESULTS AND DISCUSSION

5.1 Expected broad-band emission

Fig. 3 shows the resulting broad-band spectral energy distributions calculated for Hydra A and MS 0735.6+7421. Fig. 4 compares the expected γ -ray emission for the three outbursts considered here. The predicted HE and VHE γ -ray flux of Hydra A is the highest of the three clusters. The larger energy injected in CRs in the other two systems does not compensate for their larger distance (see Fig. 4). The last column of Table 1 shows the flux expected around 10 GeV (F'_v) under the assumption that the total energy in CR hadrons is equal to $3P_{\text{ext}}V$, i.e. $X_{\text{CR}} = 1$. For Hydra A, four curves are shown, for different assumptions on the distribution of target material and the energy in CRs: (a) $X_{\text{CR}} = 1.0$, $\eta = 1$ implying very cold material inside the bubbles, (b) $X_{\text{CR}} = 1.0$ with no gas within the bubbles, (c) $X_{\text{CR}} = 0.5$, $\eta = 2$ and (d) as for (b) but with $P_{\text{ext}}V = 4.1 \times 10^{60}$ erg rather than the 9×10^{60} erg used for the other curves. The two estimates for $P_{\text{ext}}V$ in Hydra A come from different approaches, a shock model (Nulsen et al. 2005b) and summing the $P_{\text{ext}}V$ contributions of individual bubble components (Wise et al. 2007) and can both be considered valid estimates of the outburst energetics. We find that EBL absorption in the case of Hydra A becomes important above 1 TeV. In the most distant system MS 0735.6+7421, EBL absorption is already severe above about 200 GeV and the expected γ -ray flux drops dramatically at higher energies.

Secondary electrons resulting from the p–p collisions will lead to the production of electromagnetic signals via interactions with magnetic and radiation fields. For computing the observational signature associated with secondary electrons in Hydra A, we use a

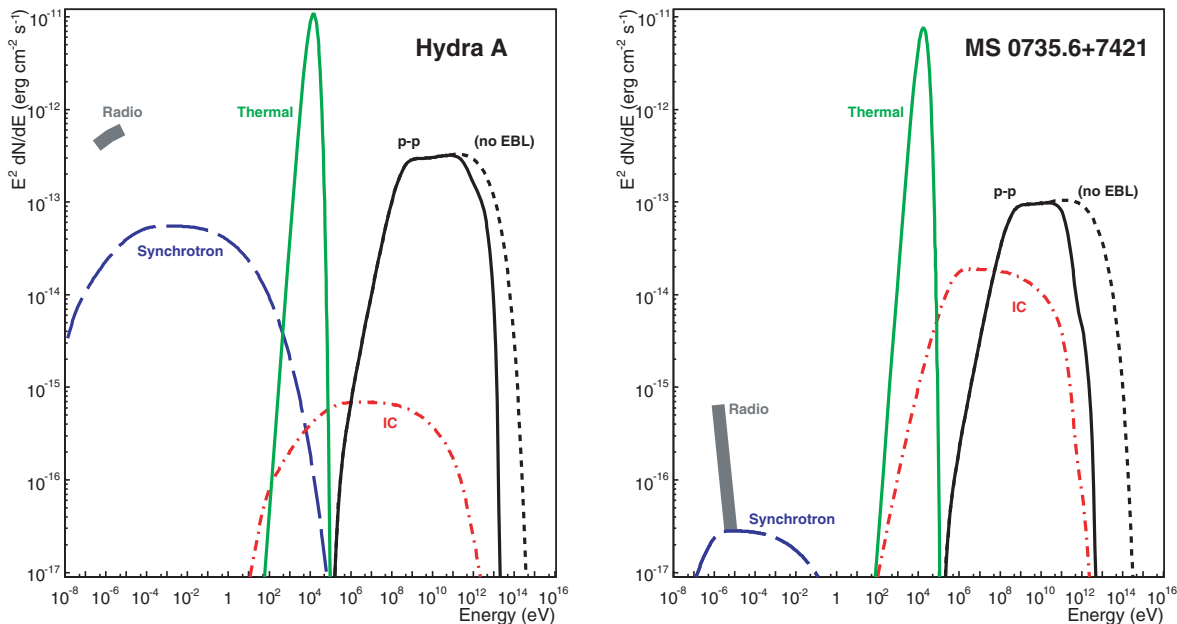


Figure 3. Model spectral energy distributions for Hydra A (left-hand panel) and MS 0735.6+7421 (right-hand panel). γ -ray emission arising from the decay of pions produced in hadronic interactions is shown with (solid line) and without (dashed line) the effect of EBL absorption. The inverse Compton and Synchrotron radiations of secondary electrons and positrons are calculated assuming magnetic field strengths of 30 and 0.13 μG for Hydra A and MS 0735.6+7421, respectively. The CMB is assumed to be the dominant target photon field for inverse Compton scattering. Radio data are taken from Lane et al. (2004) and Cohen et al. (2005).

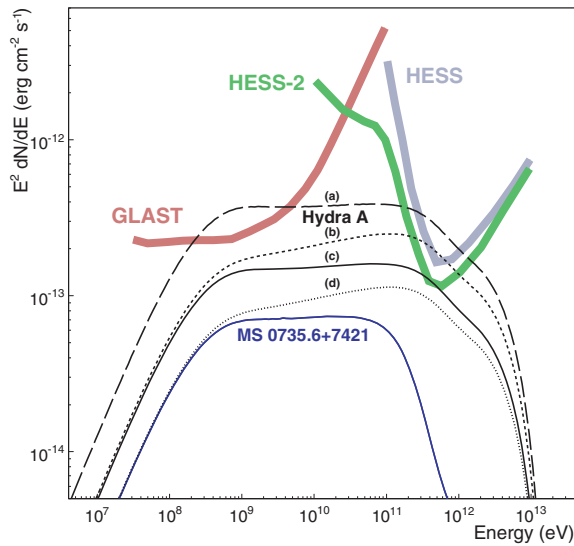


Figure 4. Predicted γ -ray emission for the most powerful known AGN outbursts. Model curves are compared to the nominal sensitivities of the GLAST, HESS and HESS-2 γ -ray detectors, for 5 yr and 50 h observations, respectively. For Hydra A four curves are shown: (a) $X_{\text{CR}} = 1.0$, $\eta = 1$ implying very cold material inside the bubble, (b) $X_{\text{CR}} = 1.0$ with no gas within the bubbles, (c) $X_{\text{CR}} = 0.5$, $\eta = 2$ and (d) as for (b) but with $P_{\text{ext}}V = 4.1 \times 10^{60}$ erg rather than the 9×10^{60} erg used for the other curves.

magnetic field of 30 μG (Taylor & Perley 1993) and inverse Compton upscattering by the CMBR only. We note that the magnetic field of relevance here is that in the regions where most target material exists, that is, just outside the bubbles. We can compare the expected synchrotron emission in the radio band with the observed level of radio flux (Lane et al. 2004) since, in principle, our model could be tested by the expected synchrotron signal from secondary electrons. However, the observed radio emission seems to be associated with primary electrons; exceeding the expectation for secondaries by a factor of ~ 50 . In the 2–10 keV X-ray band, the thermal emission of the Hydra-A lobes $\sim 10^{-11}$ erg cm^{-2} s^{-1} (Edge, Stewart & Fabian 1992) exceeds our predicted secondary synchrotron emission by three orders of magnitude (see the left-hand panel of Fig. 3). It therefore appears that in the case of Hydra A, the emission of secondary particles is completely buried by other processes and that the GeV–TeV γ -ray range may be the only wavelength band in which the existence of energetic hadrons can be probed.

The situation is somewhat different for MS 0735.6+7421. The observed radio spectrum is very steep, particularly in the outer lobes (Cohen et al. 2005). This means that although the low-frequency emission is likely dominated by primary electrons the observed radio flux of the lobes at ~ 1 GHz is very low (~ 2 mJ) – of the same order as the predicted radio emission from secondary electrons. We find that under the assumption that the total energy in hadronic CRs is equal to $3P_{\text{ext}}V$ that a B -field of > 130 nG would produce a high-frequency hardening of the radio spectrum which is not observed (see the right-hand panel of Fig. 3). A value of ~ 130 nG (the upper limit in this scenario) is rather low for the central region of a cluster and lies three orders of magnitude below the value of equipartition with relativistic particles (estimated by McNamara et al. 2005, as 100 μG). We note that radio observations of this object at > 1.4 GHz are highly desirable to probe the existence of secondary electrons (and hence CR hadrons) in this object.

5.2 γ -ray observability of these objects

It is clear from the above discussion that galaxy clusters which harbour extraordinarily powerful AGN are at the edge of detectability with current and near future γ -ray instruments if the observed bubbles are dominated by the pressure of relativistic particles ($X_{\text{CR}} \simeq 1$). Hydra A is the closest cluster-scale AGN outburst known and appears to be the most promising target of this kind for γ -ray observations. Furthermore, its emission is only moderately affected by EBL absorption in the VHE γ -ray regime. Our calculations show that, depending on the detailed properties of the source, it may be detectable using the currently operating HESS instrument and the upcoming GLAST mission. With detections from both instruments, it might be possible to determine the shape of the spectrum of CR protons in this system. Additionally, the extended γ -ray emission expected from Hydra A could be resolved by instruments such as HESS, but is not sufficiently extended to significantly degrade the detection sensitivity with respect to the point-source case. A γ -ray detection of Hydra A would provide a clear signature of hadronic CR dominance of the bubble pressure.

The situation is less auspicious for the other two examples of cluster-scale AGN outbursts. Both systems are more powerful than Hydra A but their distances make detection of a γ -ray signal more difficult. Furthermore, their larger redshifts compared to Hydra A imply rather severe absorption by the EBL, making a > 1 TeV detection of these objects extremely difficult. It is very likely that these systems can only be detected with the next generation of γ -ray telescopes (both ground based and space borne).

ACKNOWLEDGMENTS

We would like to thank Felix Aharonian, Heinz Völk, Olaf Reimer and Werner Hofmann for very useful discussions, Sven van Loo for his careful reading of the manuscript and an anonymous referee for very constructive comments. JAH is supported by a PPARC Advanced Fellowship.

REFERENCES

- Aharonian F. A., 2002, MNRAS, 332, 215
- Aharonian F. A. et al., 2006, Nat, 440, 1018
- Atayan A. M., Völk H. J., 2000, ApJ, 535, 45
- Berezinsky V. S., Blasi P., Ptuskin V. S., 1997, ApJ, 487, 529
- Biermann P. L., Strittmatter P. A., 1987, ApJ, 322, 643
- Birzan L., Rafferty D. A., McNamara B. A., Wise M. W., Nulsen P. E. J., 2004, ApJ, 607, 800
- Blanton E. L., Sarazin C. L., McNamara B. R., Wise M. W., 2001, ApJ, 558, L15
- Blanton E. L., 2004, in Reiprich T., Kempner J., Soker N., eds, The Riddle of Cooling Flows in Galaxies and Clusters of Galaxies. Charlottesville, Virginia, USA, p. 181.
- Böhringer H., Voges W., Fabian A. C., Edge A. C., Neumann D. M., 1993, MNRAS, 264, L25
- Choi Y., Reynolds C. S., Heinz S., Rosenberg J. L., Perlman E. S., Yang J., 2004, ApJ, 606, 185
- Churazov E., Forman W., Jones C., Böhringer H., 2000, A&A, 356, 788
- Celotti A., Fabian A. C., 1993, MNRAS, 264, 228
- Cohen A. S., Clarke T. E., Feretti L., Kassim N. E., 2005, ApJ, 620, L5
- Colafrancesco S., Blasi P., 1998, ApJ, 9, 227
- Dennison B., 1980, ApJ, 239, L93
- De Young D. S., 2006, ApJ, 648, 200
- Dole H. et al., 2006, A&A, 451, 417
- Dunn R. J. H., Fabian A. C., 2004, MNRAS, 355, 862
- Dunn R. J. H., Fabian A. C., Celotti A., 2006, MNRAS, 372, 1741

- Edge A. C., Stewart G. C., Fabian A. C., 1992, *MNRAS*, 258, 177
- Enßlin T. A., Biermann, P. L., Kronberg, P. P., Wu X.-P., 1997, *ApJ*, 477, 560
- Fabian A. C., 1994, *ARA&A*, 32, 277
- Fabian A. C., Celotti A., Blundell K. M., Kassim N. E., Perley R. A., 2002, *MNRAS*, 331, 369
- Fabian A. C., Sanders J. S., Allen S. W., Crawford C. S., Iwasawa K., Johnstone R. M., Schmidt R. W., Taylor G. B., 2003, *MNRAS*, 344, L43
- Feretti L., Brunetti G., Giovannini G., Kassim N., Orrù E., Setti G., 2004, *J. Korean Astron. Soc.*, 37, 315
- Fletcher R. S., Gaisser T. K., Lipari P., Stanev T., 1994, *Phys. Rev. D*, 50, 5710
- Fusco-Femiano R., Orlandini M., Brunetti G., Feretti L., Giovannini G., Grandi P., Setti G., 2004, *ApJ*, 602, 73
- Gabici S., Blasi P., 2003, *ApJ*, 19, 679
- Gabici S., Blasi P., 2004, *ApJ*, 20, 579
- Giovannini G., Feretti L., 2000, *New Astron.*, 5, 335
- Gitti M., Feretti L., Schindler S., 2006, *A&A*, 448, 853
- Gitti M., McNamara B. R., Nulsen P. E. J., Wise M. W., 2007, *ApJ*, 660, 1118
- Hinton J. A., 2004, *New Astron. Rev.*, 48, 331
- Inoue S., Aharonian F. A., Sugiyama N., 2005, *ApJ*, 628, L9
- Kaiser C. R., Pavlovski G., Pope E. C. D., Fangohr H., 2005, *MNRAS* 359, 493
- Kelner S. R., Aharonian F. A., Bugayov V. V., 2006, *Phys. Rev. D*, 74, 034018
- Kirk J. G., Guthmann A. W., Gallant Y. A., Achterberg A., 2000, *ApJ*, 542, 235
- Krennrich F. et al., 2004, *New Astron. Rev.*, 48, 345
- Landau L. D., Lifschitz E. M., 1995, *Fluid Mechanics*, Butterworth-Heinemann Ltd., Oxford
- Lane W. M., Clarke T. E., Taylor G. B., Perley R. A., Kassim, N. E., 2004, *AJ*, 127, 48
- Loeb A., Waxman, E., 2000, *Nat*, 405, 156
- Lorenz E., 2004, *New Astron. Rev.*, 48, 339
- McNamara B. R. et al., 2001, *ApJ*, 562, L149
- McNamara B. R., Nulsen P. E. J., Wise M. W., Rafferty D. A., Carilli C., Sarazin C. L., Blanton, E. L., 2005, *Nat*, 433, 45
- Nulsen P. E. J., Hambrick D. C., McNamara B. R., Rafferty D. A., Birzan L., Wise M. W., David L. P., 2005a, *ApJ*, 625, 9
- Nulsen P. E. J., McNamara B. R., Wise M. W., David L. P., 2005b, *ApJ*, 628, 629
- Owen F. N., Eilek J. A., Kassim N. E., 2000, *ApJ*, 543, 611
- Pavlovski G., Kaiser C. R., Pope E. C. D., Fangohr H., 2007, *MNRAS*, submitted (arXiv: 0709.1790)
- Pfommer C., Enßlin T. A., 2004, *A&A*, 413, 17
- Reimer O., Pohl M., Sreekumar P., Mattox J. R., 2003, *ApJ*, 588, 155
- Rephaeli Y., Gruber D., 2002, *ApJ*, 597, 587
- Reynolds C. S., McKernan B., Fabian A. C., Stone J. M., Vernaleo J. C., 2005, *MNRAS*, 357, 242
- Robinson K. et al., 2004, *ApJ*, 601, 621
- Ryu D., Kang H., Hallman E., Jones T. W., 2003, *ApJ*, 593, 599
- Schindler S., Castillo-Morales A., De Fillippis E., Schwope A., Wambsgans J., 2001, *A&A*, 376, L27
- Sikora M., Madejski G., 2000, *ApJ*, 534, 109
- Sutherland R. S., Dopita M. A., 1993, *ApJS*, 88, 253
- Taylor G. B., Perley R. A., 1996, *ApJ*, 416, 554
- Thompson D. J., 2004, *New Astron. Rev.*, 48, 543
- Völk H. J., Aharonian F. A., Breitschwerdt D., 1996, *Space Sci. Rev.*, 75, 279
- Wise M. W., McNamara B. R., Nulsen P. E. J., Houck J. C., David L. P., 2007, *ApJ*, 659, 1153

This paper has been typeset from a $\text{\TeX}/\text{\LaTeX}$ file prepared by the author.